DOI 10.1007/s11141-022-10159-2
Radiophysics and Quantum Electronics, Vol. 64, Nos. 8–9, January–February, 2022
(Russian Original Vol. 64, Nos. 8–9, August–September, 2021)

MICROWAVE RADIOMETRIC SENSING OF CUMULUS CLOUDINESS FROM SPACE

D. P. Egorov,[1*] Ya. A. Ilyushin,[2] and B. G. Kutuza[1]

UDC 504.32

We consider the Planck model for generating random discontinuous cloud fields in a three-dimensional computation domain. An algorithm for calculating a two-dimensional pattern of the brightness temperature of the upwelling microwave radiation of the smooth water surface–cloudy atmosphere system taking into account the altitude profiles of the main meteorological parameters and an arbitrary distribution of the water content is developed. The inverse problem of retrieving the distributions of the integral water-content parameters by the two-frequency radiometric method using the obtained brightness temperatures is discussed. Systematic errors in the estimated integral water content of the clouds associated with the use of a homogeneous plane-layered model of the cloud field, which ignores its actual, i.e., discontinuous and heterogeneous structure, are studied.

1. INTRODUCTION

The super-high frequency (SHF) radiometric method allows one to estimate such integral parameters as the total mass of water vapor and the water content of clouds using the brightness temperature of atmospheric radiation [1–3]. During ground-based observations of downwelling radiation, the element of the spatial resolution of the SHF radiometer is usually much smaller than the cloud size, which allows us to study the spatiotemporal variability of the atmospheric moisture-content field [4–6]. At the same time, the spatial resolution of modern satellite-borne SHF radiometers in the frequency range 10–40 GHz amounts to 12–30 km, which considerably exceeds horizontal dimensions of the cumulus clouds. When solving the inverse problem, we usually use a homogeneous plane-layered model, which ignores the properties of the discontinuous and inhomogeneous structure of the cloud field. With allowance for the nonlinear dependence of the brightness temperature of the atmosphere on the cloud water content, this feature leads to systematic errors when determining the above-given integral parameters.

This work considers the Planck model of a cloud field [7], which allows one to take the discontinuous structure of the cumulus cloudiness into account. The possibilities of its application in the problems of remote atmospheric sensing are discussed. Direct numerical simulation of the upwelling radiation of the discontinuous atmospheric cloud fields, which are generated under various values of the model parameters, is performed. In particular, this allows us to estimate the influence of the cloud cover and the size of the chosen antenna-resolution element on the error when determining the integral water content averaged over the scanning region.

* dobrix95@gmail.com

[1] V. A. Kotel'nikov Institute of Radioengineering and Electronics of the Russian Academy of Sciences; [2] M. V. Lomonosov Moscow State University, Moscow, Russia. Translated from Izvestiya Vysshikh Uchebnykh Zavedenii, Radiofizika, Vol. 64, Nos. 8–9, pp. 625–634, August–September 2021. Russian DOI: 10.52452/00213462_2021_64_08_625 Original article submitted September 21, 2021; accepted October 15, 2021.

2. SIMULATION OF RANDOM CLOUD FIELDS AND BRIGHTNESS TEMPERATURES

The field of random discontinuous cloudiness can be generated according to the Planck model [7] with specified cloud distribution over the diameters and single-valued coupling of the vertical extent of each cloud with its diameter. Using the results of processing of a large base of stereoscopic photographs of cloudiness in the region of Florida peninsula, USA, Planck proposed the following formula in 1969:

$$n(D) = K \exp(-\alpha D), \qquad 0 \le D \le D_{\mathrm{m}}. \tag{1}$$

Here, D is the cloud diameter, $n(D)$ is the number of the clouds with the diameters ranging from D to $\mathrm{d}D$, D_{m} is the maximum diameter of a cloud in the set, K is the normalization coefficient, and α is a parameter depending on the time of the day and various local climatic environments.

The relation between the vertical length H and the diameter D of the cloud has the form

$$H = \eta \left(\frac{D}{D_{\mathrm{m}}}\right)^{\beta}, \tag{2}$$

where η and β are the dimensionless parameters [7].

Note that there also exist other models of the fields of discontinuous cloudiness. Thus, the following distribution of the clouds by the diameters is proposed in [8] on the basis of the results of processing the aircraft-borne measurements carried out in Ukraine:

$$n(D) = KD \left(1 - \frac{D}{D_{\mathrm{m}}}\right)^{p_0}, \qquad 0 \le D \le D_{\mathrm{m}}, \tag{3}$$

where p_0 is the distribution parameter which amounts to 4.35 on the average. Here, the coefficient K has the dimension of the inverse square of the length as distinct from (1) in which it has the dimension of the inverse length.

We confine ourselves to considering convective clouds of the cumulus type. The average values of the effective temperature, water content, thickness, and the altitude of the lower boundary of the clouds Cu hum/med/cong are given in [1, 9]. The altitude profile of the water content of such a cloud can be calculated using the following formula [10–12]:

$$\widetilde{w}(\xi) = \widetilde{w}(\xi_0)\frac{\xi^{\mu_0}(1-\xi)^{\psi_0}}{\xi_0^{\mu_0}(1-\xi_0)^{\psi_0}} = \frac{W}{H}\frac{\Gamma(2+\mu_0+\psi_0)}{\Gamma(1+\mu_0)\Gamma(1+\psi_0)}\xi^{\mu_0}\left(1-\xi\right)^{\psi_0}, \tag{4}$$

where $\xi = h/H$ is the reduced height inside the cloud, H is the cloud thickness, W is the (integral) water content of the cloud, $\widetilde{w}(\xi)$ is the water-content profile inside the cloud, $\widetilde{w}(\xi_0)$ is the maximum water content of the cloud, with ξ_0 as the reduced altitude of the maximum water content, μ_0 and ψ_0 are the dimensionless parameters, and $\Gamma(\zeta)$ is the gamma function. According to [1], $\mu_0 = 3.27$, $\psi_0 = 0.67$, and $\xi_0 = 0.83$, and the dependence of the water content W on the extent H of a cumulus cloud is roughly approximated by the following formula using the tabulated data, which are given in [1]:

$$W[\mathrm{kg/m^2}] = 0.132574(N[\mathrm{km}])^{2.30215}. \tag{5}$$

To carry out the calculation experiment, we specify the calculation region $\Omega \in Oxyz$ with an area of 50×50 km (the scanning region), the altitude 10 km (along the Oz axis) and a grid of $300 \times 300 \times 500$ nodes. The cloud shape is assumed to be cylindrical. The location C of any cloud in Ω is given by the coordinates of the center of its lower base $O_C = x_C, y_C, z_C$. It is also assumed that the cloud boundaries do not intersect and cannot be located one above another. In this case, according to Eqs. (1) and (2), we conclude that the plane structure of the cloud field (in its vertical projection onto the plane Oxy) depends only on the values of the model parameters K, D_{m}, and α with accuracy up to the chosen coordinates x_C and y_C for each cloud. The three-dimensional structure of the cloud field is influenced not only by the above-given parameters, but also β, η, and z_C, which is the altitude of the lower boundary of the cloud. However, within the framework of this study, the coordinate z_C is assumed to be the same and equal to 1.5 km for all clouds for the sake of simplicity.

Having specified the values of the model parameters K, D_{m}, α, β, and η, we generate the field of the discontinuous cumulus cloudiness. The quantitative distribution of the clouds over the diameters is obtained from Eq. (1) replacing D by the quantity $kD_{\mathrm{m}}r^{-1}$, where k is the integer, $1 \le k \le r$, and r is chosen using the parameters of the available computation grid. For example, it may be assumed that $r = \sqrt{i_*^2 + j_*^2}$, where i_* and j_* are the numbers of the grid nodes falling within the distance D_{m} along the directions Ox and Oy, respectively.

The selection of the coordinates x_C and y_C, i.e., the location, is carried out sequentially for each cloud C using a random-number generator (with uniform distribution), but with allowance for the verification of the condition of nonintersection of the boundaries of C with all other clouds for which the location has already been found. In this case, the clouds are sorted in advance in descending order of their diameters. The numerical experiment shows that with such an iterative filling of the area Ω with clouds, in an acceptable time of searching for a suitable random location for each new cloud, it is possible to achieve the maximum percentage of coverage of the plane $h = 0$ with clouds (intensity) at a level of 60–65% without the involvement of the specialized algorithms for optimal packaging. However, we have failed to reach a higher filling percentage.

Having generated the cloudiness field, at each point of the plane of the zero height, $h = 0$, we define the water-content profile $w(h)$, such that $w(h) = \widetilde{w}[(h - H_0)/H]$ (see Eq. (4)), if h is located inside the cloud with the lower-boundary height H_0 and thickness H and $w(h) = 0$, if h is located outside the cloud. To calculate the brightness temperatures, in addition to the water-content profile, one should know the altitude profiles of the thermodynamic temperature $T(h)$, the atmospheric pressure $P(h)$, and the air humidity $\rho(h)$. Let us use the standard atmospheric model with the exponential laws of the altitude distribution of the temperature, pressure, and humidity. The brightness temperature of the thermal radio radiation of the system atmosphere–underlying surface (upwelling in the direction θ, $0 \le \theta \le 0.4\pi$), which is recorded for the horizontal (h) or vertical (v) polarization at a certain frequency ν, can be written as follows (the subscripts ν in the formula are omitted for simplification):

$$T_j^*(\theta) = T^{\uparrow}(\theta) + T_s\kappa_j(\theta)\exp[-\tau(0)\sec\theta] + T^{\downarrow}(\theta)R_j(\theta)\exp[-\tau(0)\sec\theta]. \tag{6}$$

Here, $j = \mathrm{v}, \mathrm{h}$ and the atmosphere is assumed to be a layered and horizontally homogeneous medium,

$$T^{\downarrow}(\theta) = \int\limits_0^{\infty} T(h)\gamma(h)\sec\theta\,\exp\left[-\int\limits_0^{h}\gamma(z)\sec\theta\,\mathrm{d}z\right]\mathrm{d}h \tag{7}$$

is the brightness temperature of the atmospheric downwelling radiation (the corresponding expression for the upwelling radiation differs only by the integration limits), h is the height, $\gamma(h)$ is the linear absorption coefficient, which is combined over all atmospheric components, $T(h)$ is the height profile of the thermodynamic temperature, $\tau(0)$ is the total absorption in zenith ($\theta = 0°$), $R_j(\theta)$ is the reflection coefficient of the surface (a function of polarization), $\kappa_j(\theta)$ is the radiation coefficient of the surface ($\kappa_j(\theta) = 1 - R_j(\theta)$ on the assumption of local thermodynamic equilibrium), and T_s is the thermodynamic temperature of this surface.

In the case of a smooth water surface [1, 13], the reflection coefficient $R_j(\theta)$ can be expressed in terms of the complex permittivity ε of water. Introducing the sliding angle $\psi = 90° - \theta$, we write

$$R_j(\theta) = R_j(90° - \psi) = |M_j(\psi)|^2, \tag{8}$$

where

$$M_{\mathrm{h}}(\psi) = \left[\sin\psi - \left(\varepsilon - \cos^2\psi\right)^{0.5}\right]\left[\sin\psi + \left(\varepsilon - \cos^2\psi\right)^{0.5}\right]^{-1}, \tag{9}$$

$$M_{\mathrm{v}}(\psi) = \left[\varepsilon \sin\psi - \left(\varepsilon - \cos^2\psi\right)^{0.5}\right] \left[\varepsilon \sin\psi + \left(\varepsilon - \cos^2\psi\right)^{0.5}\right]^{-1}. \tag{10}$$

If $\theta = 0°$ and, obviously, $\psi = 90°$ then (9) and (10) degenerate:

$$M_{\mathrm{v}} = -M_{\mathrm{h}} = \left(\varepsilon^{0.5} - 1\right) \left(\varepsilon^{0.5} + 1\right)^{-1}. \tag{11}$$

The permittivity ε is a function of the radiation frequency ν (or the wavelength λ) and the thermodynamic temperature t of water (in the case under consideration, $t = T_{\mathrm{s}}$) and can be written in the following form [1, 14]:

$$\varepsilon = \varepsilon_{\mathrm{O}} + \frac{\varepsilon_{\mathrm{S}} - \varepsilon_{\mathrm{O}}}{1 + \Delta\lambda^2} - i\,\Delta\lambda\,\frac{\varepsilon_{\mathrm{S}} - \varepsilon_{\mathrm{O}}}{1 + \Delta\lambda^2}, \qquad \Delta\lambda = \frac{\lambda_{\mathrm{S}}}{\lambda}. \tag{12}$$

Here, ε_{O} is the "optical" component of permittivity, $\varepsilon_{\mathrm{S}} = \varepsilon_{\mathrm{S}}(t)$ is the "static" component, $\lambda_{\mathrm{S}} = \lambda_{\mathrm{S}}(t)$ is the characteristic wavelength, which is related to the relaxation time of the water molecules. The temperature dependences for the parameters ε_{O}, ε_{S}, and λ_{S} can be found, e.g., in [1, 15], which also have corrections to the values of these parameters for nonzero salinity.

The combined linear absorption coefficient $\gamma(\nu, h)$ can be written as the sum

$$\gamma[\mathrm{Np/km}](\nu, h) = \gamma_{\mathrm{O}}^*[\mathrm{Np/km}](\nu, h) + \gamma_{\rho}^*[\mathrm{Np/km}](\nu, h) + \gamma_{w}^*[\mathrm{Np/km}](\nu, h), \tag{13}$$

where γ_{O}^* and γ_{ρ}^* are the linear absorption coefficients in oxygen and water vapor, respectively, and γ_{w}^* is the linear absorption in a cloud. The former two coefficients can be approximated by the theoretical-empirical dependences $\gamma_{\mathrm{O}}[\mathrm{dB/km}](\nu, h) = \gamma_{\mathrm{O}}[\mathrm{dB/km}][\nu, T(h), P(h)]$ and $\gamma_{\rho}[\mathrm{dB/km}](\nu, h) = \gamma_{\rho}[\mathrm{dB/km}][\nu, T(h), P(h), \rho(h)]$, which have been borrowed from the recommendations of the International Telecommunication Union [16], such that $\gamma_{\mathrm{O}}^* = \chi\gamma_{\mathrm{O}}$, whereas $\gamma_{\rho}^* = \chi\gamma_{\rho}$, where $\chi = 0.23255814$ is the coefficient of transition from decibels to Nepers (energy units).

The linear absorption γ_w in a cloud comprising only homogeneous spherical particles can be written as [17]

$$\gamma_w = 10^{-3} \int\limits_0^\infty Q_{\mathrm{o}}(a[\mathrm{m}])\, N[\mathrm{m}^{-4}](a[\mathrm{m}])\, \pi (a[\mathrm{m}])^2\, \mathrm{d}a[\mathrm{m}], \tag{14}$$

where a is the particle size (radius), $N(a)$ is the function of the particle distribution over the sizes, $Q_{\mathrm{o}}(a) = Q_{\mathrm{o}}(a, \lambda, t_w)$ is the factor of the attenuation efficiency, which also depends on the wavelength λ and the average effective temperature t_w of the cloud. For small particles when the wavelength in a particle is much greater than its size, Q_{o} has the following form [17]:

$$Q_{\mathrm{o}}(a) = \frac{8\pi a}{\lambda} \mathrm{Im}\left(\frac{\varepsilon - 1}{\varepsilon + 2}\right). \tag{15}$$

Substituting (15) into (14), we obtain

$$\gamma_w[\mathrm{nP/km}] = \frac{0.6\pi}{\lambda[\mathrm{cm}]} \mathrm{Im}\left(\frac{\varepsilon - 1}{\varepsilon + 2}\right) \int\limits_0^\infty \frac{4\pi}{3} (a[\mathrm{m}])^3 N[\mathrm{m}^{-4}](a[\mathrm{m}])\, \mathrm{d}a[\mathrm{m}] = k_w(\lambda, t_w) w, \tag{16}$$

where

$$k_w(\lambda, t_w) = \frac{0.6\pi}{\lambda[\mathrm{cm}]} K_C, \quad K_C = \mathrm{Im}\left(\frac{\varepsilon - 1}{\varepsilon + 2}\right) = \frac{3\,(\varepsilon_{\mathrm{S}} - \varepsilon_{\mathrm{O}})\,\Delta\lambda}{(\varepsilon_{\mathrm{S}} + 2)^2 + (\varepsilon_{\mathrm{O}} + 2)^2\,\Delta\lambda^2}, \tag{17}$$

K_C is the multiplier, which determines the temperature variation in a cloud. When calculating ε according to (12), it is assumed that $t = t_w$. At the same time, w is a dimensionless quantity and is understood as the liquid-droplet water content in unit volume, i. e., water content can, therefore, be expressed in $\mathrm{kg/m^3}$.

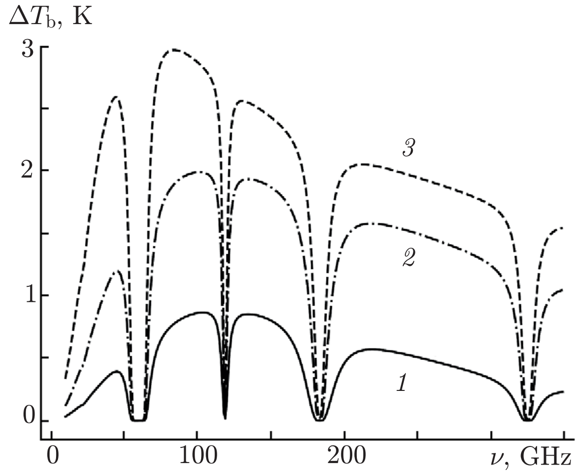

Fig. 1. The difference of the values $\Delta T_{\rm b}(\nu)$ for the frequency range ν from 10 to 350 GHz for various thicknesses H of the layer of continuous cloudiness: ($H = 1$ km *1*, $H = 2$ km *2*, and $H = 3$ km *3*) for the standard profiles $T(h)$, $P(h)$, and $\rho(h)$, smooth water surface, $T_{\rm s} = 15\,^\circ$C, and the average effective temperature of the clouds $t_w = -2\,^\circ$C.

Thus, speaking of the altitude distribution of this water content and absorption, we can write the absorption coefficient $\gamma_w^*(\nu, h)$ as the product of the weight function $k_w^*(\nu, t_w) = k_w(c\nu^{-1},\ t_w)$ and the water content $w(h)$.

Let us consider a continuous layer of clouds of the thickness $H = 1$, 2, and 3 km with the corresponding (5) integral water content. Let us compare the constant altitude profile of the water content (the water content is not changed with the height inside the cloud) and the profile specified according to Mazin (4). Let us calculate the model values of the brightness temperatures of the radiation of the system "smooth water surface–atmosphere," which upwells in the zenith direction, for both cases. Figure 1 shows the difference $\Delta T_{\rm b}(\nu)$ between these values for the frequency range from 10 to 350 GHz. The surface temperature $T_{\rm s}$ is assumed equal to $15\,^\circ$C, the salinity is zero, and the average effective temperature of the cloud is $t_w = -2\,^\circ$C. According to Fig. 1, for the same integral water content, the brightness temperature for a cloud with a constant altitude profile of the water content always exceeds the brightness temperature of the cloud whose water content is distributed in accordance with (4).

3. RETRIEVAL OF THE INTEGRAL PARAMETERS OF WATER CONTENT

The two-frequency radiometric method for determining the integral parameters of water content is given in [1, 9]. Using the atmospheric brightness temperature, which was measured only at two frequencies, it allows one to estimate the values of the total mass Q of water vapor and the water content W of the clouds. If the effective temperature t_w of the clouds is known and the total absorption in the atmospheric thickness is comparatively low ($\tau \lesssim 1$ Np), it is sufficient to write and solve the system of two equations, which are linear with respect to Q and W

$$\tau_{\nu_i}[\mathrm{Np}] = \tau_{\rm O}(\nu_i) + k_\rho(\nu_i)\, Q[\{\mathrm{g/cm^2}] + k_w^*(\nu_i, t_w) W[\mathrm{kg/m^2}], \qquad i = 1, 2, \tag{18}$$

where τ_ν is the estimate of the total coefficient of the atmospheric absorption in the zenith direction, $\tau_{\rm O}(\nu)$ is the model coefficient of total absorption in oxygen [16], $k_w^*(\nu, t_w)$ is the previously introduced (see (17)) weight function of absorption in the cloud, and the expression for $k_\rho(\nu)$ can, e.g., be found in [1, 18].

In this case, the key point is to estimate the total atmospheric absorption τ_{ν_i} at the zenith (or $\tau(0)$ in the previous notations) using the known brightness temperatures at the selected frequencies. Let us use the following expressions as the approximations for the brightness temperatures of the upwelling ($T^\uparrow(\theta)$) and downwelling ($T^\downarrow(\theta)$) radiation in the direction θ:

$$T^\uparrow(\theta) = T_{\rm av}^\uparrow \Big\{1 - \exp[\tau(0)\sec\theta]\Big\}, \quad T^\downarrow(\theta) = T_{\rm av}^\downarrow \Big\{1 - \exp[\tau(0)\sec\theta]\Big\}, \tag{19}$$

where $T_{\rm av}^\uparrow$ and $T_{\rm av}^\downarrow$ are the average effective atmospheric temperatures for the upwelling and downwelling radiation, respectively, $0 \le \theta \le 0.4\pi$. Using these approximations, we substitute (19) into (6) and obtain

$$T_j^*(\theta) = T_{\rm av}^\uparrow \{1 - \exp[-\tau(\theta)]\} + T_s \kappa_j(\theta) \exp[-\tau(\theta)] + T_{\rm av}^\downarrow \{1 - \exp[-\tau(\theta)]\}\, R_j(\theta) \exp[-\tau(\theta)]. \tag{20}$$

Here, $j = \mathrm{v}, \mathrm{h}$ and $\tau(\theta)$ is understood as $\tau(0)\sec\theta$. Note that Eq. (20) is quadratic with respect to $\exp[-\tau(\theta)]$.

Solving this equation for fixed polarization, we obtain an estimate for the coefficient of total absorption

$$\exp[-\tau(\theta)] = \frac{-b+\sqrt{D}}{2a} \quad \text{or} \quad \tau(0) = \ln\left(\frac{2a}{-b+\sqrt{D}}\right)\cos\theta, \tag{21}$$

where $a = T_{\rm av}^{\downarrow}\, R_j(\theta)$, $b = T_{\rm av}^{\uparrow} - T_{\rm av}^{\downarrow}\, R_j(\theta) - T_s\kappa(\theta)$, and $D = b^2 - 4a\,[T^*(\theta) - T_{\rm av}^{\uparrow}]$.

To estimate the total absorption in the zenith, one should first estimate the average effective temperatures $T_{\rm av}^{\uparrow}$ and $T_{\rm av}^{\downarrow}$, the reflection coefficient $R_j(\theta)$, and the temperature $T_{\rm s}$ of the underlying surface. The errors when estimating these four parameters lead to an error in determining the total-absorption coefficient and, therefore, influence the Q and W retrieval accuracy. In actual experiments, the retrieval accuracy of these integral parameters is also influenced by the conceptual impossibility of an accurate calculation of $\tau_{\rm O}$ and k_ρ because of the discrepancy between the standard model profiles $T(h)$, $P(h)$, and $\rho(h)$ and the actually observed.

With allowance for Eqs. (1)–(14), we calculate two-dimensional patterns of the brightness temperature distribution of the radiation (going in the zenith direction) of the "smooth water surface–cloudy atmosphere" system at the frequencies $\nu = 22.2$ and 27.2 GHz for $K = 205$, $D_{\rm m} = 3$ km, $\alpha = 1$, $\beta = 0.5$, and $\mu = 1$. The surface temperature $T_{\rm s}$ is assumed to be equal to 15 °C. The height of the lower boundary of the clouds is fixed (1.5 km). The average effective temperature of the clouds is $t_w = -2\,^\circ$C. Using the obtained brightness-temperature distributions, we also retrieve the integral water-content pattern (see Fig. 2) with the help of the two-frequency method (15)–(18). The percentage (cover) of the cloudiness (i.e., the fraction of the $h = 0$ plane coverage by the clouds in their projection to this plane) amounted to 57.78 %. The value of the water content W^* averaged over the scanning region (50×50 km over the entire region), which was obtained by integrating the profile $w(h)$ over h at each point of the plane $h = 0$ and the subsequent averaging over all points, amounted to 0.31 kg/m^2. According to (5), a continuous cloud layer with such a water content would have a thickness of 1.44 km. However, the cloud thickness averaged over the entire area amounted only to 0.92 km.

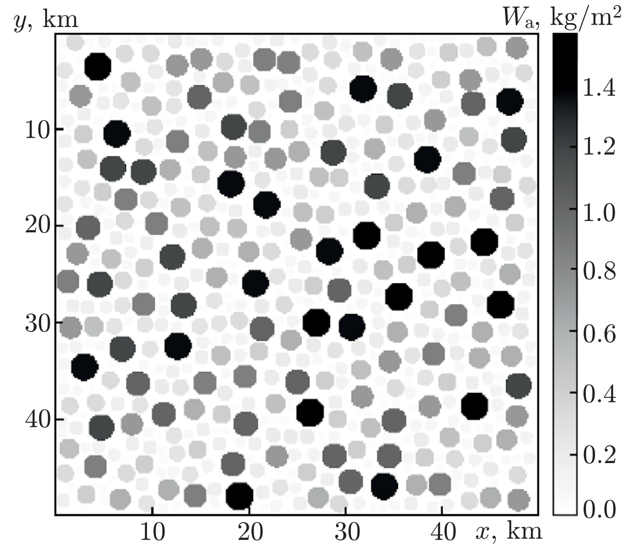

Fig. 2. The integral water content retrieved by the two-frequency (22.2 and 27.2 GHz) method using the model values of the brightness temperature of the upwelling radiation of the system "smooth water surface–cloudy atmosphere" for the standard profiles $T(h)$, $P(h)$, and $\rho(h)$, smooth water surface, $T_{\rm s} = 15\,^\circ$C, the average effective temperature $t_w = -2\,^\circ$C of the clouds, and the Planck-model parameters $D_{\rm m} = 3$ km, $\alpha = 1$, $\beta = 0.5$, $\eta = 1$, and $K = 205$.

Assuming $\theta = 0^\circ$, $T_{\rm s} = 15\,^\circ$C, and $t_w = -2\,^\circ$C, we generate the cloud fields for various K, $D_{\rm m}$, α, β, and η and calculate the arrays $T_{\rm b}^{\nu} = T_{\rm b}^{\nu}(k,l)$ of the brightness-temperature values for fixed frequencies ν. Varying the state of the random-number generator (with uniform distribution), which determines the horizontal locations of the clouds, we obtain several $\{T_{\rm b}^{\nu}\}$ for the same parameter set. To study systematic errors of retrieval of the water content (averaged over the scanning region), emerging because of using the homogeneous plane-layered model of the cloud field, which ignores its actual (discontinuous) structure, we subject the arrays of the brightness temperatures $T_{\rm b}^{\nu}$ to unit-by-unit averaging (22) with the units of $n \times n$ nodes successively for $n = 1, 2, 3 \ldots 300$ and follow the dynamics of the average values of the water content, which was retrieved according to (18)–(21):

$$\widetilde{T}_{\rm b}^{\nu}(i,j) = \sum_{k,l} \frac{T_{\rm b}^{\nu}(k,l)}{n^2}, \tag{22}$$

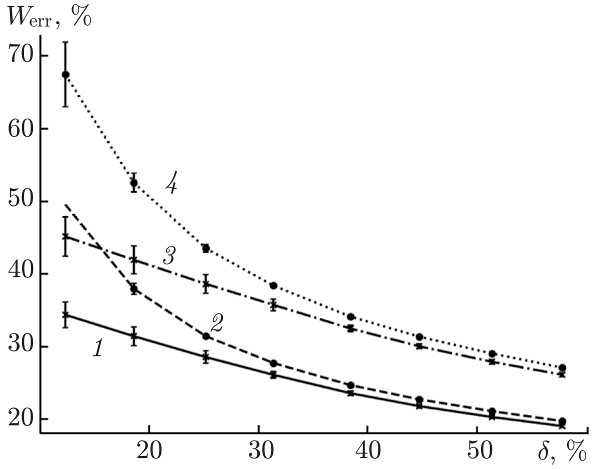

Fig. 3. The relative error $W_{\rm err}$ as a function of the cloudiness percent δ for the fixed resolution-element size $n \times n$, $n = 30$ nodes (curves *1* and *3*) and $n = 150$ nodes (curves *2* and *4*). The two-frequency method was used. The following frequency combinations were used: 22.2 and 27.2 GHz (curves *1* and *2*) and 22.2 and 37.5 GHz (curves *3* and *4*). The calculations were performed for the standard profiles $T(h)$, $P(h)$, and $\rho(h)$, the smooth water surface, $T_{\rm s} = 15\,^\circ$C, the effective cloud temperature $t_w = -2\,^\circ$C and the Planck-model parameters $D_{\rm m} = 3$ km, $\alpha = 1$, $\beta = 0.5$, $\eta = 1$, and $44 \leq K \leq 205$.

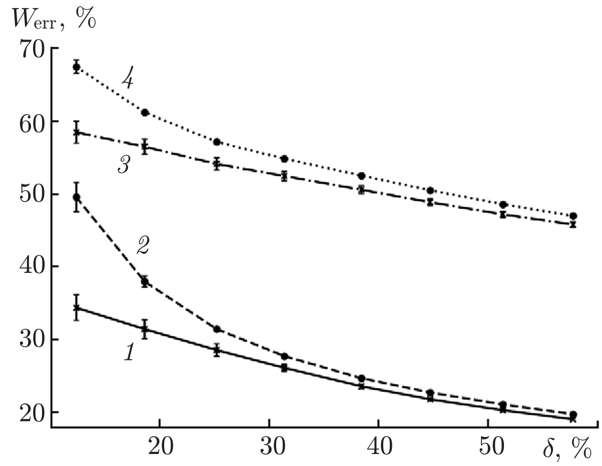

Fig. 4. The relative error $W_{\rm err}$ as a function of the cloudiness percent δ for the fixed resolution-element size $n \times n$, $n = 30$ nodes (curves *1* and *3*), $n = 150$ nodes (curves *2* and *4*). The two-frequency method was used. The following frequency combinations were used: 22.2 and 27.2 GHz (curves *1* and *2*), 22.2 and 90.8 GHz (curves *3* and *4*). The calculations were performed for the standard profiles $T(h)$, $P(h)$, and $\rho(h)$, the smooth water surface, $T_{\rm s} = 15\,^\circ$C, the effective cloud temperature $t_w = -2\,^\circ$C and the Planck-model parameters $D_{\rm m} = 3$ km, $\alpha = 1$, $\beta = 0.5$, $\eta = 1$, and $44 \leq K \leq 205$.

where $n\,i^* \leq k < n\,(i^* + 1)$, $n\,j^* \leq l < n\,(j^* + 1)$, and $i^* = [i/n]$, $j^* = [j/n]$. The square brackets denote integer division. Thus, the units have no intersections and are understood as resolution elements (averaging), with the help of which the pattern of discontinuous clouds $T_{\rm b}^{\nu}$ is reduced to a set of the plane-layered approximations $\widetilde{T}_{\rm b}^{\nu}$.

Let us fix the frequency combination (ν_1, ν_2) and, using the corresponding arrays $\widetilde{T}_{\rm b}^{\nu_1}$ and $\widetilde{T}_{\rm b}^{\nu_2}$ retrieve the two-dimensional distribution of the integral water content $W(i,j)$. The average value $W_{\rm a} = \langle W(i,j) \rangle_{i,j}$ (here, the operation $\langle \cdot \rangle_{i,j}$ denotes averaging over all i, j), which is calculated for various n by the two-frequency method, is compared with the "actual" average water content W^*, which, as previously, is obtained by direct integration of the profile $w(h)$ over h at each point of the plane $h = 0$ and subsequent averaging over all points. The relative error $W_{\rm err}$ is introduced by the standard method:

$$W_{\rm err} = \frac{|W^* - W_{\rm a}|}{W^*} \cdot 100\ \%. \tag{23}$$

The dependence of the relative error $W_{\rm err}$ on the cloudiness percent is given in Figs. 3 and 4 for various frequency pairs ($\nu_1$andν_2) for the fixed resolution element $n \times n$, i.e., 30×30 nodes (correspond to the region 5×5 km), curves *1* and *3* and 150×150 nodes (25×25 km), curves *2* and *4*. The Planck-model parameters are $D_{\rm m} = 3$ km, $\alpha = 1$, $\beta = 0.5$, and $\eta = 1$. The altitude of the lower boundary for all clouds amounts to 1.5 km. The parameter K controls the cloudiness percent and varies in the interval from 44 to 205. For each iteration over K, the random-number generator, which determines the horizontal locations of the clouds, was started 100 times for various initial conditions. The confidence intervals in Figs. 3 and 4 reflect the corresponding spread of the values.

According to the numerical experiment, as the cloudiness percent decreases, i.e., as the cloudiness-field discontinuity increases, starting from $n \geq 10$ nodes, one can observe a pronounced increase in the value of the relative error W_{err} when determining the integral water content, such that this error increases at a higher rate for a larger resolution element. An increase in the resolution element n always leads to an increase in W_{err} for any fixed percentage (cover) of the clouds.

4. CONCLUSIONS

We have realized the Planck model for generating the discontinuous cloud fields in the three-dimensional calculation region [19]. The numerical experiment on calculating the two-dimensional distributions of the brightness temperature of the upwelling (in the zenith direction) radiation of the "smooth water surface–cloudy atmosphere" system at frequencies of 22.2, 27.2, 37.5, and 90.8 GHz under the conditions of discontinuous cloudiness has been carried out. Systematic errors when retrieving the integral water content because of the failure to allow for the discontinuous structure of cumulus clouds have been analyzed. It is shown that the relative error of determining (by the radiometric method) the value of the water content of the clouds averaged over the scanning region significantly increases with increasing discontinuity of the cloud field. The size of the chosen element of the spatial resolution (of the antenna), using which, the discontinuous pattern of the cloudiness is reduced to a set of plane-layered approximations, is of great importance.

The obtained results testify to a necessity of allowance for the structure and discontinuity of the clouds when processing the satellite data and solving the inverse problem of determining the atmospheric characteristics. In the performed experiments under conditions of 60% cloudiness of moderate vertical development, if the discontinuity factor is ignored, the error of determining the water content (averaged over the region 50×50 km) using the two-frequency radiometric method with the resolution element 5×5 km and the frequency combination 22.2 and 27.2 GHz (the best one out of those considered) amounts to about 20%. This is the best indicator since the error still increases with increasing resolution-element sizes and, especially, decreasing cover. Additional quantitative and qualitative data on the clouds can be obtained using the satellite measurements in the visible, infrared, and terahertz ranges. Optical instruments observe the upper layer of the clouds and determine their mask, altitude, and temperature. This helps us allow for not only the discontinuity of the clouds, but also other factors. Knowledge of the spatial structure of the upper level also makes it possible to identify the zones of frontal and convective clouds, which can be used in the subsequent targeted processing of the satellite microwave radiometric data. Nevertheless, the issue of practical use of the results obtained in the work requires further study.

This work was carried out using the equipment of the Shared core facility of the superhigh-capacity computational resources of M. V. Lomonosov Moscow State University [20] and under the support of the Ministry of science and higher education of the Russian Federation (State assignment No. 0030–2019–0008 "Kosmos").

REFERENCES

1. B. G. Kutuza, M. V. Danilychev, and O. I. Yakovlev, *The Satellite Monitoring of the Earth: Microwave Radiometry of the Atmosphere and the Surface* [in Russian], LENAND, Moscow (2016).
2. A. E. Basharinov and B. G. Kutuza, *Trudy GGO im. A. I. Voeikov*, No. 222, pp. 100–110.
3. A. E. Basharinov, S. T. Egorov, M. A. Kolosov, and B. G. Kutuza, *Trudy GGO im. A. I. Voeikov*, No. 222, pp. 153–158.
4. D. P. Egorov and B. G. Kutuza, *IEEE Trans. Geosci. Rem. Sens.*, **59**, No. 5, 605–617 (2021). https://doi.org/10.1109/TGRS.2020.3034533
5. D. P. Egorov and B. G. Kutuza, *J. Phys. Conf. Ser.*, **1632**, 012010 (2020). https://doi.org/10.1088/1742-6596/1632/1/012010

6. D. P. Egorov, B. G. Kutuza, and M. T. Smirnov, *Photonics and Electromagnetics Research Symposium. Proc. June 17–20, 2019, Rome, Italy*, pp. 3421–3427. https://doi.org/10.1109/PIERS-Spring46901.2019.9017620
7. V. G. Planck, *J. Appl. Met.*, **8**, No. 1, 46–67 (1969). https://doi.org/10.1175/1520-0450(1969)008<0046:TSDOCC>2.0.CO;2
8. I. P. Mazin and S. M. Shmeter, eds., *Cumulus Clouds and the Related Deformation of the Meteoelement Fields* [in Russian], Trudy. TsAO, No. 134 (1977).
9. A. B. Akvilonova and B. G. Kutuza, *Radiotekh. Elektron.*, **23**, No. 9, 1792–1806 (1978).
10. I. P. Mazin and S. M. Shmeter, *Clouds, Structure and Formation Physics* [in Russian], Gidromteoizdat, Leningrad (1983).
11. I. P. Mazin and S. M. Shmeter, *Cloud-Physics Issues* [in Russian], Gidromteoizdat, Leningrad (1978).
12. F. Yu. Voit and I. P. Mazin, *Izv. AN SSSR, Fiz. Atm. Okeana*, **8**, No. 11, 1166–1176 (1972).
13. B. G. Kutuza and M. T. Smirnov, *Issled. Zemli Kosm.*, No. 3, 76–83 (1980).
14. F. T. Ulaby, R. K. Moore, and A. K. Fung, *Microwave Remote Sensing. Active and Passive, Vol. 1*, Addison-Wesley Pub. Com., London (1981).
15. V. I. Rozenberg, *Scattering and Attenuation of Electromagnetic Radiation by Atmospheric Particles* [in Russian], Gidrometeoizdat, Leningrad (1972).
16. ITU-R P.676-3. *Attenuation by Atmospheric Gases (Question ITU-R 201/3).* International Telecommunication Union (1997).
17. H. C. Hulst, *Light Scattering by Small Particles*, Dover Publications Inc., New York (1981).
18. D. P. Egorov, Ya. A. Ilyushin, Ya. V. Koptsov, and B. G. Kutuza, *J. Phys. Conf. Ser.* 1991??, 012015 (2021). https://doi.org/10.1088/1742-6596/1991/1/012015
19. https://github.com/dobribobri/meteo-
20. Vl. V. Voevodin, S. A. Zhumatiy, S. I. Sobolev, et. al, *Otkr. Sist. SUBD*, No. 7, 36–39 (2012).